On the evolution of aerosol properties at a mountain site above Mexico City

D. Baumgardner,[1,2] G. B. Raga,[1] G. Kok,[2] J. Ogren,[3] I. Rosas,[1] A. Báez,[1] and T. Novakov[4]

Abstract. Size distributions, scattering and absorption coefficients, and the bulk chemical composition of aerosols have been measured at a mountain site 400 m above the southwest sector of the Mexico City basin during a two-week period in November 1997. Variations in these properties are primarily related to local meteorology, i.e., wind direction and relative humidity; however, a link was found between carbon monoxide and ozone and the partitioning of aerosols between Aitken and accumulation mode sizes. Relative humidity was also found to affect this partitioning of aerosol size and volume. In addition, the fraction of sulfate in the aerosols was much higher on a high-humidity day than on a very low humidity day; however, the fraction of the mass contained in organic and elemental carbon was the same regardless of humidity levels. The daily variations of aerosol properties are associated with the arrival of new particles at the research site transported from the city basin and their subsequent mixture with aged aerosols that remain in the residual layer from the night before.

1. Overview

Aerosol particles in urban areas are a major issue with respect to their impact on public health, damage to the environment, and changes to regional and global climate. The mutagenic and carcinogenic effects due to human inhalation of urban aerosols, particularly those composed of carbon, have been shown in numerous epidemiological studies [e.g., *Dockery et al.*, 1992, 1993; *International Agency for Research on Cancer (IARC)*, 1989; *Pitts*, 1983; *Schuetzle*, 1983]. Recent studies have also shown that atmospheric aerosols can significantly alter photochemical production rates of ozone; for example, ozone formation can be enhanced as a result of light scattering by aerosols [*Dickerson et al.*, 1997] or suppressed if actinic fluxes are decreased by aerosol layers that absorb radiation [*Raga and Raga*, 2000]. When aerosol particles are exported from their urban source regions, they contribute to the regional and global background of natural aerosols, where they may play a role in regional or global climate changes as they alter radiative fluxes or change the physical or optical properties of clouds.

Numerous observational and modeling studies of aerosols have been conducted in major cities in industrial countries like the United States and Germany, but only recently has similar attention been focused on major urban areas in other parts of the world, particularly in developing countries [*Cahill et al.*, 1996; *Knox*, 1996; *Mage et al.*, 1996; *World Health Organization, United Nations Environment Programme, (WHO UNEP)*, 1992]. The air quality situation in megacities like Mexico City underlines the need for comprehensive gas and aerosol studies in the world's developing countries. The daily maximum ozone level of this metropolis, with a population of 18 million, exceeds the Mexican ozone standard of 110 ppbv more than 300 days out of the year. Mexican authorities have taken major steps to reduce pollution levels, e.g., greatly reducing industrial sources of sulfur dioxide (SO_2), requiring the use of unleaded fuel and catalytic converters, and enforcing mandatory no-drive days. The ozone levels and aerosol loading, however, are still well above acceptable standards, and more action will be necessary if the air quality is to be brought into compliance with standards.

There is sparse information about the physical or optical properties of Mexico City aerosols. The city has a network of 36 sites that measure CO, SO_2, NO_x, O_3, and PM_{10} (particulate matter having an aerodynamic diameter of 10 μm or less; tapered element oscillating microbalance (TEOM) method). There are no published data on the size-differentiated physical, optical, or chemical properties. Several past studies have analyzed the chemical composition of Mexico City aerosols captured on filters (*Aldape et al.* [1991a, 1991b], *Cahill et al.* [1996], *Miranda et al.* [1992], *Seila et al.* [1993], and, more recently *Edgerton et al.* [1999]), but these were from filters where the particle mass was dominated by coarse mode aerosols, i.e., mechanically generated particles like dust or road debris. A more detailed analysis of aerosol physical and chemical properties, especially in the submicron size range, is necessary to understand how these aerosols form and evolve.

The scarcity of information about the physical characteristics of Mexico City aerosols motivated a project in November 1997 to study the formation and growth of these particles. One objective was to acquire detailed size distributions, size-resolved particle composition, and bulk optical properties, i.e., absorption and scattering coefficients, as the first step in the creation of a database of information on Mexico City aerosols. The complementary objective was to evaluate the relationship of aerosol properties to precursor gases like CO and SO_2 and other environmental factors, e.g., water vapor, temperature, and winds. The present paper summarizes the properties of

[1]Centro de Ciencias de la Atmósfera, Universidad Nacional Autónoma de México, Mexico City.
[2]National Center for Atmospheric Research, Boulder, Colorado.
[3]National Oceanic and Atmospheric Administration, Boulder, Colorado.
[4]Lawrence Berkeley Laboratory, University of California, Berkeley.

aged aerosols that originate in Mexico City and discusses how changes in these properties relate to local meteorology and chemistry.

2. Project Description

The experimental site was located within the Mexico City Ecological Reserve (19°15′N, 99°11′W), in the southwest corner of the Mexico City basin, at an elevation 440 m above the average city level of 2240 m. Most of the analysis in the following discussions has been constrained to those time periods when the wind is from the north so as to exclude potential aerosol sources closest to the research site and focus on the more aged aerosol from the city basin. The closest, major source of aerosols and gases is an eight-lane, perimeter freeway around the south and west edges of the city that is in a direct line, approximately 2 km north, but 200–300 m below the site.

Measurements of carbon monoxide (CO), sulfur dioxide (SO_2), total reactive nitrogen (NO_y), and ozone (O_3) were made once per second, 24 hours a day. Pressure, temperature, humidity, wind, and scattering and absorption coefficient measurements were also made continuously, but averaged into 1 min intervals. A differential mobility analyzer (DMA) measured particle size spectra in the size range from 0.01 to 0.7 μm (one spectrum every 6 min) from 0700 to 1900 local standard time (LST) every day. The exception was the time period from November 15 to 16 when the measurements were continued throughout the night. The total concentration and volume from 0.01 to 0.7 μm are derived by integrating the size distribution from the DMA. Cascade impactors (Andersen and MOUDI) captured particles on Teflon and aluminum substrates that were subsequently analyzed to determine particle mass and chemical composition as a function of particle size. The impactor foils were exposed from 1000 to 1700 LST every day, the period when the site was normally in the polluted mixed layer. The aerosols measured by the DMA and impactors were not dried before sampling; however, the sheath air in the DMA was dried prior to mixing with the aerosol stream.

The total scatter coefficient σ_s was measured at three wavelengths (450, 550, and 700 nm) with a nephelometer. The absorption coefficient σ_a was measured with a particle soot absorption photometer (PSAP). Particles were first passed through a 1 μm cut-size impactor and heated to insure a relative humidity less than 40% before these optical properties were measured. The PSAP measurements were corrected for light scattering and other effects that bias the absorption measurements using the suggested factors of *Bond et al.* [1999].

Visible and ultraviolet solar radiation were measured with hemispheric radiometers, and the pollution layer evolution was recorded by time-lapsed video (1 frame per minute) and digital camera (1 picture every 30 min).

The equipment was installed in rooms on the second floor of a building within the reserve. All gas and aerosol samples, except the Andersen impactor samples, were taken from air brought through a chimney with a fan that maintained a flow rate of approximately 90 L m^{-1}. The chimney extended above the building by approximately 2 m and a total of approximately 8 m above the ground. The Andersen impactor was located on a patio outside the second-floor equipment room. The meteorological and radiation measurements were made at approximately the same elevation as the top of the chimney. Figure 1 illustrates the general layout of instrumentation inside and
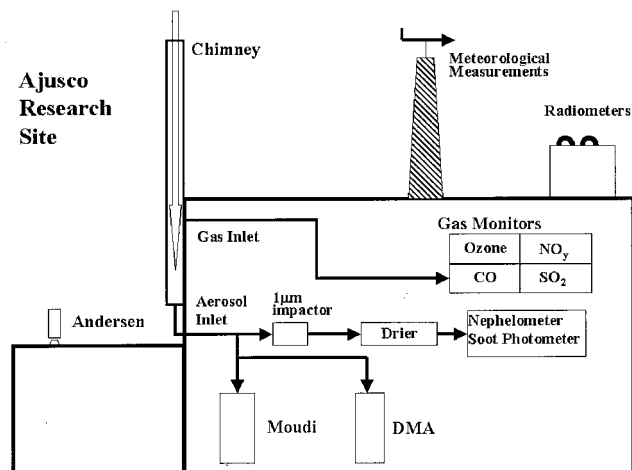

Figure 1. The general layout of instrumentation and measurement sites is shown in this schematic. The research station is a two-story house with a balcony extending from the second floor. The Andersen impactor measurements were made from this balcony. All other aerosol and gas measurements were made inside the house on samples taken from air brought down a chimney. Meteorological and radiation measurements were made from the roof of the house.

outside the research site. For the analysis of this paper the measurements were processed into 6 min averages that corresponded to the accumulation interval of the DMA. Table 1 lists the specifications and estimated uncertainties of the sensors whose measurements are discussed in this paper.

The field campaign extended from November 6 to 18, 1997, a period that is normally near the end of this region's rainy season. The meteorological, radiation, gas, impactor, and DMA measurements started on the morning of November 6. The scattering and absorption measurements began on the afternoon of the following day.

3. Results

The principal focus of the field campaign was to investigate the physical properties of aerosols transported from the city. There were no measurements of these properties within the city, i.e., at the emission source, so we are unable to directly evaluate formation and growth processes. As will be shown, however, an analysis of daily trends in the optical and physical properties of the particles measured at the research site provides useful information about aerosol evolution when linked with the local meteorology and gas tracers of the city air. Sections 3.1–3.3 present the daily trends observed in the meteorology and tracer gases and their relationship to features of the aerosol size distributions.

3.1. Daily Trends

Figure 2 illustrates the time history of UV radiation, wind direction, relative humidity (RH), CO, O_3, aerosol concentrations ($<1 \mu$m), σ_s and σ_a during the research period. The local meteorology during the project has been discussed in detail by *Raga et al.* [1999a]. In brief, the winds at the research site (Figure 2b) move down the mountain slope (southwesterly) at night and in the early morning but shift northeasterly by midmorning as the hillside is heated by the sun. There is a transitional period for several hours as the winds bring fresh emis-

Table 1. Measured Parameters and Measurement Systems

Parameter	Measurement Method/Sensor Manufacturer	Range and Accuracy
O_3	UV absorption, TECO Inc.	0–1 ppmv ± 15%
NO	chemiluminescence, TECO Inc.	0–1 ppmv ± 25%
NO_y	chemiluminescence, TECO Inc.	0–1 ppmv ± 25%
SO_2	pulsed fluorescence, TECO Inc.	0–500 ppbv ± 15%
CO	gas filter correlation, TECO Inc.	0–10 ppmv ± 15%
UV radiation	hemispheric pyranometer, Eppley Inc.	0.295 μm to 0.385 μm, 0–60 Wm^{-2} ± 1.5%
Solar radiation	hemispheric pyranometer, Eppley Inc.	0.285 μm to 2.80 μm, 0–1400 Wm^{-2} ± 1.5%
Temperature, humidity, pressure, and winds	Davis Instruments Inc., meteorological station	−50° to +50° ± 1°, 0–100% ± 5%, 100–1024 mbar ± 1 mbar
Aerosol mass	Andersen seven-stage impactor with quartz filters; gravimetric analysis with Sartorius analytical balance	±5 μg
Aerosol ion composition	ion chromatography	only positive ions were identified with qualitative results
Aerosol carbon mass	thermal separation of impactor foils taken with a MOUDI sampler and conversion of absorption measurements made with soot photometer	estimated accuracy approximately ±50%
Aerosol size distribution	TSI SMPS system, with model 3080 electrostatic classifier and model 3025A ultrafine condensation nuclei (CN) counter	0.010 μm to 0.7 μm ± 10%
Total and back scattering coefficient	TSI model 3563 nephelometer, 450, 550, and 700 nm wavelengths	1–1000 Mm^{-1}, estimated accuracy ~10%
Absorption coefficient	particle soot absorption photometer, 565 nm wavelength, Radiance Research	1–100 Mm^{-1}, estimated accuracy ~30%

sions up the slopes but before the mixed layer has risen above the site. This is normally indicated by an abrupt increase in the CO mixing ratios within minutes after the wind shift followed by a secondary increase in CO as the top of the mixed layer rises above the site. The mixed layer thickness is typically 1–2 km [*Raga et al*., 1999a], lifting the top of the layer 600–1000 m above the measurement point. The half-hourly photographs give evidence that the top of the mixed layer usually rose above the research site by 1000 or 1100 LST. Figure 3 depicts a typical time sequence of the polluted mixed layer development, starting at 0715 LST and continuing until 1315 LST. The top of the mixed layer appears quite sharp early in the morning as a result of the low sun angle and concentration of pollutants in a shallow layer. The edge of this layer becomes less distinct throughout the morning, finally losing its definition as the research site becomes immersed. In late afternoon, with sunlight no longer on the hillsides, the wind once again shifts and moves down the hillside.

The CO measurement is an indicator of the degree of mixing that occurs from initial emission in the city basin, approximately 2 km upwind, to the point of measurement. A network of 36 gas-monitoring stations is maintained by the city and measures CO, O_3, NO_x, and SO_2. The primary sink of CO is oxidation by OH to CO_2. As this is a relatively slow reaction, the only other mechanism by which CO is decreased is by dilution as the boundary layer grows during the day. A comparison of daily, average maximum values of CO within the city to the CO measured at the research site showed that the CO normally decreased by a factor of 2 or 3, depending upon the amount of solar heating and wind speeds [*Raga et al*., 1999a]. Figure 2 shows a number of interesting features when other parameters are compared to the CO levels. At night, CO al-

most always decreases to much lower than daytime values, i.e., <0.5 ppm. The O_3, σ_a, and σ_s (Figures 2e, 2g, and 2h), however, often remain quite high throughout the evening and early morning. For example, from the evening of November 15 to morning of November 16, O_3 never decreased below 50 ppb. Likewise, σ_a and σ_s remained above 6×10^{-5} and 5×10^{-4}, respectively. Thus the processes responsible for the removal of CO were apparently not removing either ozone or particles.

The decrease in UV radiation and increase in RH reflect a period from November 8 through November 11 when there were heavy clouds caused by a tropical depression several hundred kilometers to the southwest. There were also several occurrences of fog, drizzle, and rain on November 9 and 10. The O_3 during this period of disturbed weather remained much lower because of the decreased UV; however, the CO, σ_a, and σ_s values were higher than at any other time during the project. These meteorologically contrasting periods offer an opportunity to evaluate aerosol properties under conditions of low and high humidity, as will be presented below in section 3.3. First, however, we examine the daily variations in the physical and optical properties of the aerosols.

3.2. Daily Evolution of Aerosol Properties

Some of the properties that describe an aerosol population's characteristics are chemical composition, the size distributions, and the light absorption and scattering coefficients. As described in section 2, the composition and mass of the aerosols were determined by ion chromatography and gravimetric analysis, respectively. Aerosol mass is dominated by coarse mode particles, i.e., particles that are mechanically generated such as wind-blown dust or road debris from vehicular traffic. This is illustrated in Figure 4 where the total mass is shown for each
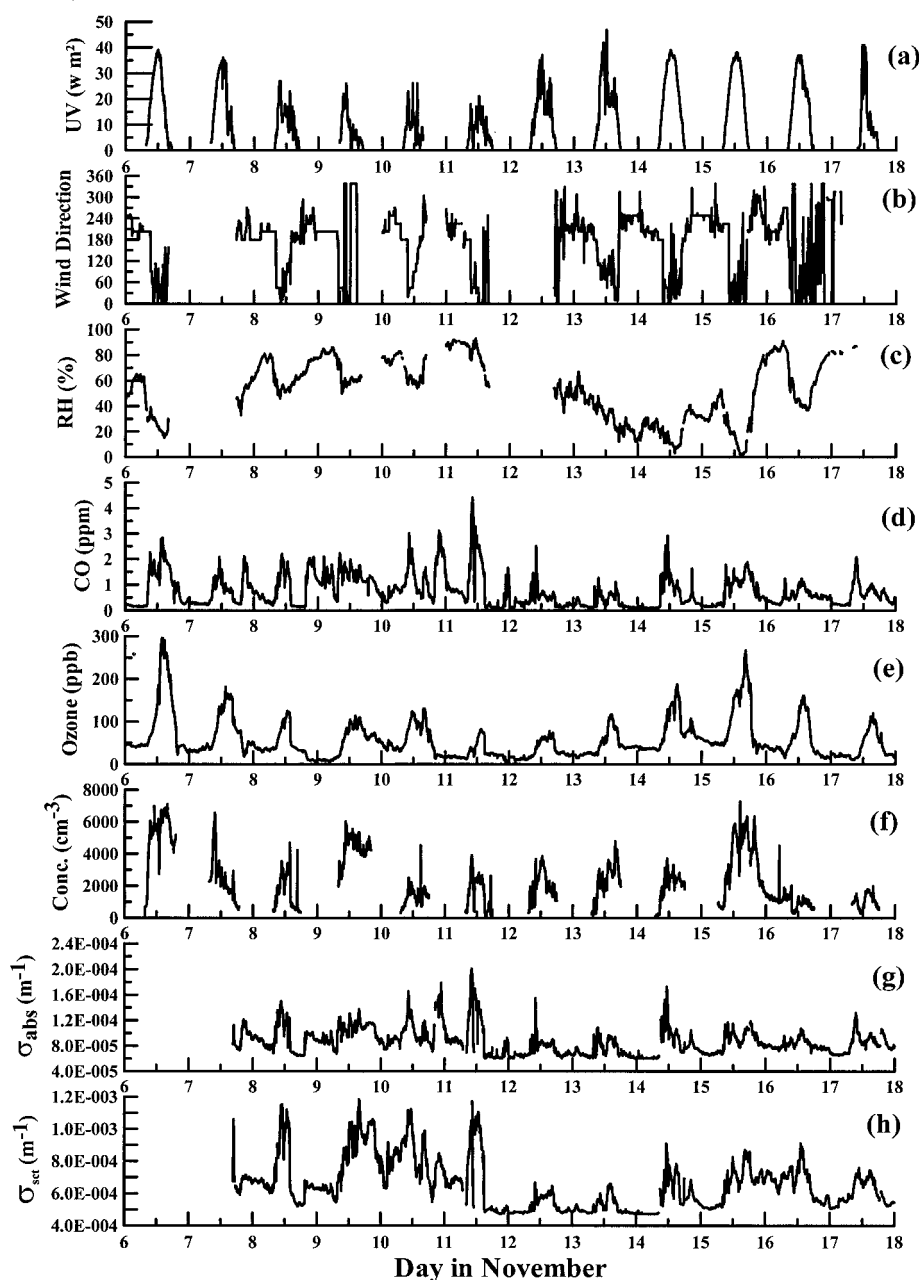
Figure 2. These time histories of (a) UV, (b) wind direction, (c) relative humidity, (d) CO, (e) O_3, (f) aerosol concentration, (g) absorption coefficient, and (h) scattering coefficient illustrate the diurnal variations.

of the research days except November 9, when no samples were taken. The "total mass" represents the sum of mass from all the impactor stages, while the "small mass" is from stages 5–8, i.e., diameters less than 3.3 μm. The small mass is an approximation of the mass derived from conventional $PM_{2.5}$ samplers, with their 2.5 μm size cut. The Andersen impactor does not collect particles with diameters less than 0.43 μm, so the "total" does not reflect the full size spectrum of particles. Figure 4 shows large day-to-day variability in the total mass, ranging from 50 to 170 μg m^{-3}. This is expected since the large-particle population that dominates the total mass varies with the local meteorology in the basin, particularly the wind speed, which was quite variable throughout the research period. The small-particle mass is less variable with a range from

40 to 60 μg m^{-3}. This suggests a more constant source of smaller particles, less dominated by the meteorology and more related to local anthropogenic emissions.

The distribution of particle sizes can be represented by displaying the number or volume of particles that have sizes within selected size categories, as illustrated in Figure 5 from DMA measurements during November 6. The DMA classifies the particles into 62 size categories; however, we have combined these 62 bins into 18 to produce a statistically significant number of counts in each size bin. These size bins are of unequal sizes; therefore the concentrations and volumes in each size bin have been normalized by the base 10 logarithm of the bin width. The size distribution in Figure 5b is the number concentration as a function of size, and the Figure 5a shows the
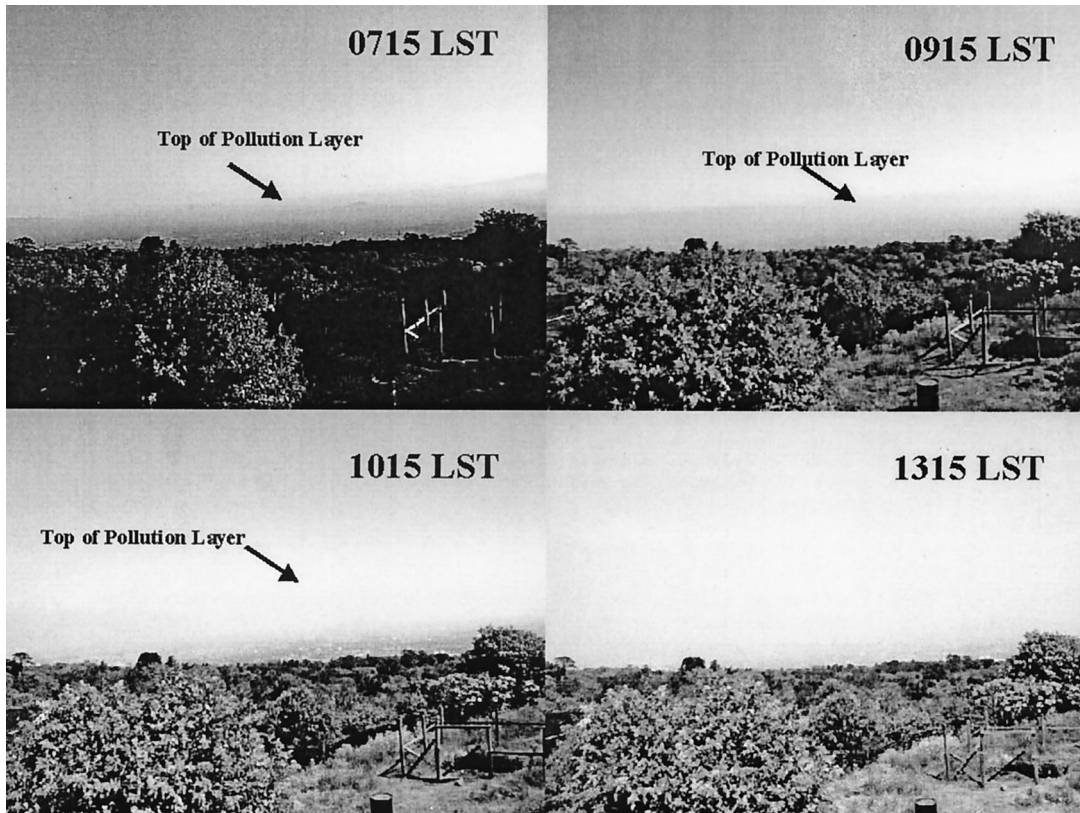
Figure 3. The development of the vertical structure of the Mexico City pollution layer is shown in this series of photographs taken during the day of November 6, 1997. The top of the mixed layer is approximately at the same level as the research site by 1015 LST. By 1315 LST the top of the mixed layer can no longer be discriminated from the photographs, and the city features are also obscured.

volume distribution. The ordinate is scaled logarithmically; hence the areas under the curves are the total concentration or volume. Two distributions are shown in each graph: one averaged over the morning transition period and the other during
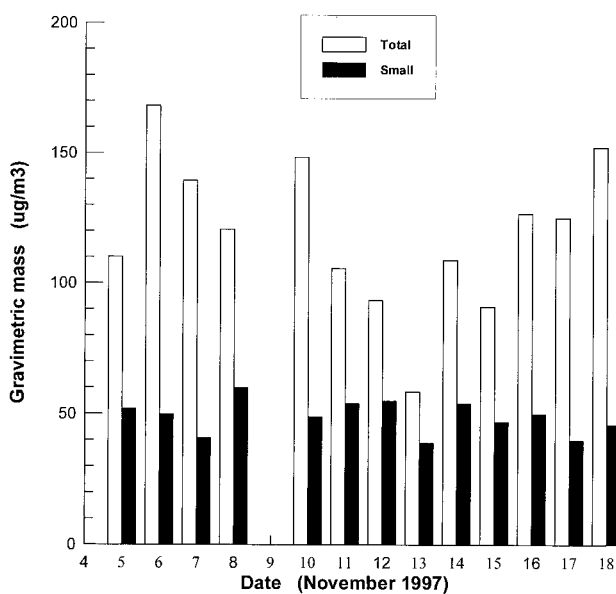
Figure 4. The daily total (<10 μm) and small (<3.3 μm) particle mass concentrations are shown here with the open and solid bars, respectively.

the mixed layer period, illustrating that both the number and volume distributions change during the course of the day.

Rather than show sequences of size distributions to describe daily variations and changes throughout the project, it is expedient to simplify the presentation by finding parameters that can describe these changes without the need to display the complete shape of the distributions. Aerosol populations are oftentimes classified into several size ranges or modes: Aitken (or nucleation), accumulation, and coarse. This classification is based upon the processes by which aerosols form and evolve. The Aitken mode particles cover the diameter range from 0.01 μm to 0.1 μm and are typically formed by homogeneous or heterogeneous nucleation. Particles in the accumulation mode range from 0.1 to 1 μm in diameter and normally evolve from Aitken mode particles that are growing by coagulation or condensation. Particles larger than 1.0 μm fall in the coarse mode category and, as discussed in section 1, are mechanically generated. In the following discussion, only the measurements from the DMA will be used, i.e., those particles that fall in the Aitken and accumulation mode size ranges.

The relative concentration and volume of particles in the Aitken and accumulation mode size ranges are indicators of the underlying processes that form and transform the aerosol population. An increase in the relative concentration and volume of Aitken particles might suggest new particle formation or a change in air mass. Likewise, an increase in the relative concentration of accumulation mode particles could indicate a changing air mass or an increase in particle mass growth rate. The parameters used in the following analysis are the Aitken
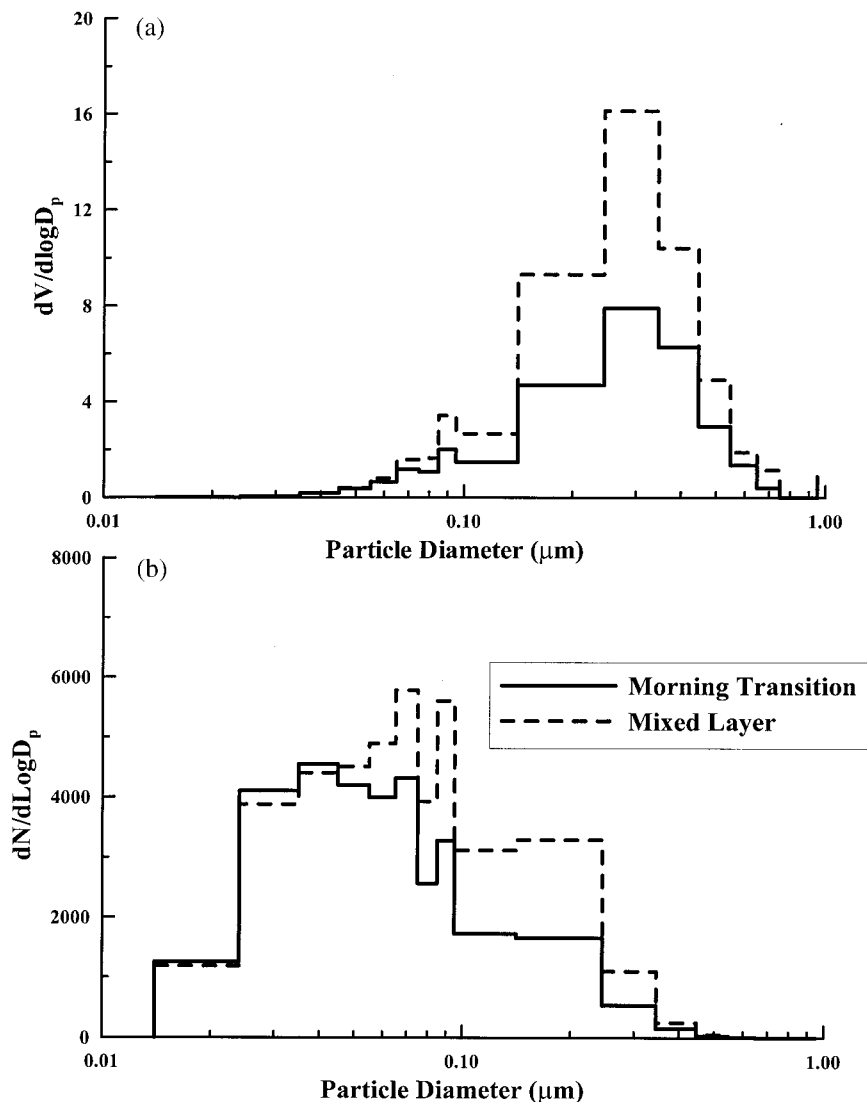
Figure 5. These graphs are examples of particle size distributions arranged by (a) volume and (b) number concentration measured with the differential mobility analyzer. The distributions are averages during the morning transition (solid curves) and mixed layer (dashed curves) periods of November 6.

mode concentration and volume fractions C_{Aik} and V_{Aik}, respectively, and the accumulation mode concentration and volume fractions C_{acc} and V_{acc}. These are calculated by dividing the particle concentrations and volumes in a given size range by the total concentration or volume over the total size range measured by the DMA (0.01–0.7 μm). Hence $C_{acc} = 1 - C_{Aik}$ and $V_{acc} = 1 - V_{Aik}$.

Figure 6 shows the variation of these parameters throughout the project in comparison to CO, O_3, total number concentration, and scattering coefficient. This time series shows systematic variations during the day and over larger timescales that appear to be linked to similar variations in O_3 and σ_s at the same scales. In almost all cases, on a daily basis, C_{Aik} and V_{Aik} increase from their initial values until they reach a maximum near midday after which they either decrease or remain more or less constant. During the majority of the days they undergo a secondary increase from midafternoon until sampling was terminated. The DMA was operated over one and a half diurnal cycles from 0700 LST on November 15 to 1900 LST on

November 16. In this time period, C_{Aik} reaches a minimum at midnight of November 15, and conversely, C_{acc} reaches its maximum. Since this is the only period in which there are 24 hour data from the DMA, it cannot be concluded that this trend is necessarily typical of every day. The general feature, however, seen in the trends of C_{Aik} and C_{acc} suggests that the nighttime trends seen on November 15 and 16 might be fairly typical.

On a larger temporal scale the maximum values of C_{Aik} and V_{Aik} show a trend that is negatively correlated with the maximum values of O_3 and σ_s. From Figure 2 we see that this large-scale trend is also related to periods of higher and lower humidity whereby the peak C_{Aik} and V_{Aik} values occur during the driest periods of the research period.

An additional link was found between CO and the aerosol optical properties, σ_s and σ_a. As shown in Figure 7, there are linear relationships between these optical properties and CO. Both correlation coefficients are statistically significant at a confidence level greater than 99%. These data were con-
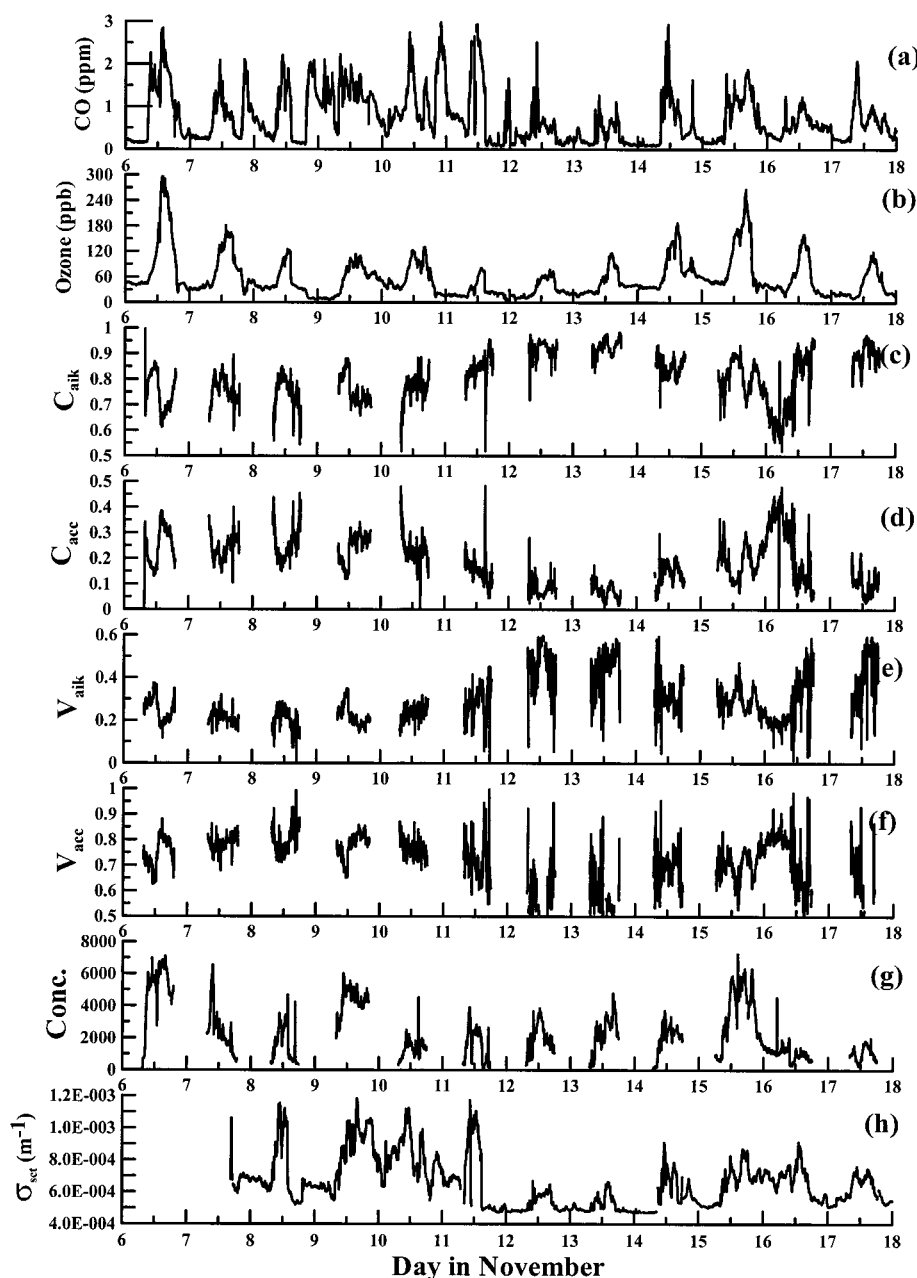
Figure 6. These time histories of (a) CO, (b) ozone, (c) Aitken mode concentration fraction, (d) accumulation mode concentration fraction, (e) Aitken mode volume fraction, (f) accumulation mode volume fraction, (g) concentration, and (h) scattering coefficient illustrate the daily variations in aerosol properties related to changes in tracers of city air (CO and ozone).

strained to time periods when the air at the research site should have been only from the city basin, i.e., when the wind direction was from −30° to 45°.

3.3. Relative Humidity Effects

The measurements were further stratified to evaluate differences that might be attributed to changes in the relative humidity, since the time series (Figures 2 and 6) showed similar trends in aerosol properties and RH. The aerosol properties were evaluated for two cases, RH < 50% and RH > 60%. The hygroscopicity of urban aerosols is largely unknown at this time, but for the analysis it was assumed that aerosols at RH

less than 50% contain little water but will be partially hydrated when RH is greater than 60%. As discussed in section 2, optical and DMA measurements were made after particles were dried, so any differences between low and high RH will be a result of processes that occurred as a result of the presence of water vapor and not because of water in the particles at the time of measurement. An additional constraint was to restrict the analysis to particles in air coming from the city, using the criteria discussed in section 3.2.

Figure 8 presents frequency distributions of σ_s, σ_a, C_{Aik}, V_{Aik}, C_{acc}, V_{acc}, total concentration, and total volume for the low- and high-RH cases. The effect on total concentration is

σ_{abs} Vs CO $r^2 = 0.84$

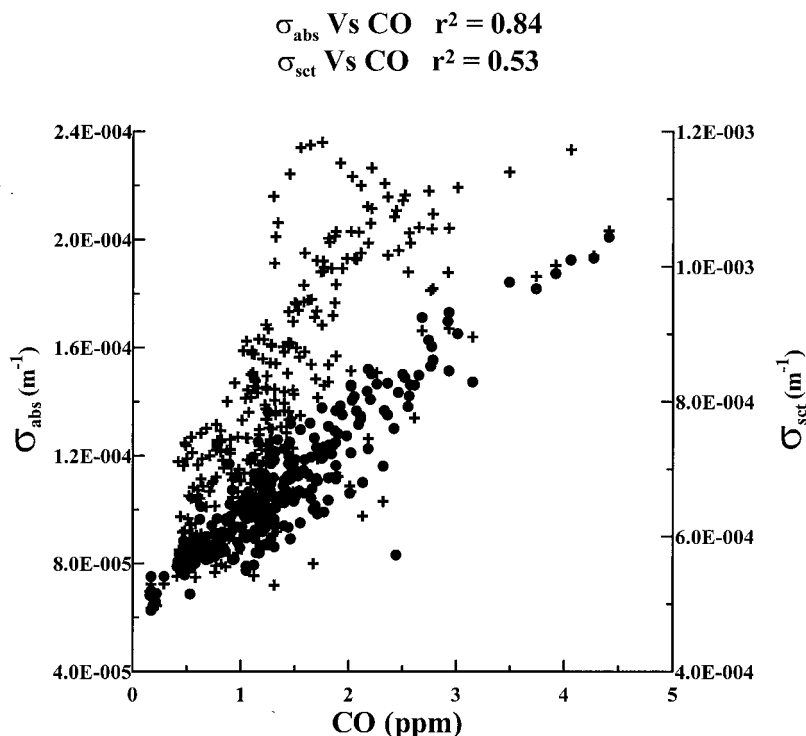σ_{sct} Vs CO $r^2 = 0.53$

Figure 7. The absorption (solid circles) and scattering (crosses) coefficients are compared to CO measurements for all time periods when the air at the research site is primarily from the city basin, i.e., wind speed >0.5 ms^{-1} and direction $-30°-45°$. Both of the correlation coefficients (r^2) are statistically significant with a confidence level >99%. Read 2.4E-004 as 2.4×10^{-4}.

slight, and the only noticeable effect on the total volume is the appearance of a secondary peak at 5 μm^3 cm^{-3} in the case of higher RH. The principal impact of higher humidity is found in the partitioning of concentration and volume between Aitken and accumulation modes. C_{acc} and V_{acc} increase with higher RH, an increase that is reflected by a significant increase in the scattering coefficients, σ_s and σ_a.

The impact on chemical composition of the particles was examined by selecting 2 days that represented extremes in RH, November 10 and 14, with very high and very low RH levels, respectively. The ion analysis of the Andersen samples for the low- and high-RH days showed sulfate as the primary negative ion found in the particles. As shown in Figure 9 the total sulfate mass on the particles is significantly larger on the high-RH day (32 μg m^{-3}) than for low RH (6 μg m^{-3}).

For these same 2 days the mass fraction of organic carbon (OC) and elemental carbon (EC) was estimated by combining measurements of σ_a with analysis of impactor samples. The total mass of EC was derived from σ_a by assuming that the EC had a specific absorption of 10 m^2 g^{-1}. This value was chosen with two major assumptions. First, it assumes that the source of primary soot particles is high-temperature combustion, e.g., diesel engines. The optical and physical properties of this type of particle have been well characterized [e.g., *Goldberg*, 1985]. Second, we assume that the particles on the PSAP filters represent a polydisperse composite of sizes, 10% carbon by mass. The specific absorption, taken from recent studies [*Fuller et al.*, 1999], can vary as much as ±20%, depending upon the carbon mass mixing ratio and the assumed geometric mean of the particle size distribution. The relative fraction of OC and EC in the total carbon was derived by thermoseparation [*Novakov*,

1981] whereby evolved carbon dioxide was measured while foils from the different stages of the MOUDI impactor were heated in a stepwise fashion in the presence of oxygen. The distribution of evolved carbon versus temperature is used to distinguish organic carbon (OC) from elemental carbon (EC). Carbon mass above a temperature of 500° is assumed to be elemental, and any mass at lower temperatures is OC. This method has uncertainties from a number of sources [*Novakov*, 1981], and at best, the absolute concentration accuracy is ±50%. The relative accuracy for comparison between the 2 days, however, is probably better, and the uncertainty is estimated as less than ±25%. The derived total carbon measured on both days was ≈13 μg m^{-3}. The elemental carbon for the low- and high-RH days was 3.7 and 4.5 μg m^{-3}, respectively.

Figure 10 summarizes the proportions of sulfate and carbon in the aerosol particles for the two cases. Samples were also analyzed for nitrates, but no significant concentrations were found, consistent with the results of *Edgerton et al.* [1999] for PM-2.5 measurements. The total mass concentrations of particles less than a micrometer were 30 and 35 μg m^{-3} for the low- and high-RH days, respectively. The fraction of EC (13%) and OC (28%) in the particles was approximately the same on both days. The principal difference in the 2 days is the shift in relative mass concentrations of sulfate and "other" particles. The high-RH day sulfate fraction is a factor of 20 larger than that on the low-RH day. The low-RH day has a factor of 3 more mass in the "other" particles than in the high-RH case. Since filters were only analyzed for some inorganic ions and total carbon (TC), it is not possible to determine what the "other" category may be.
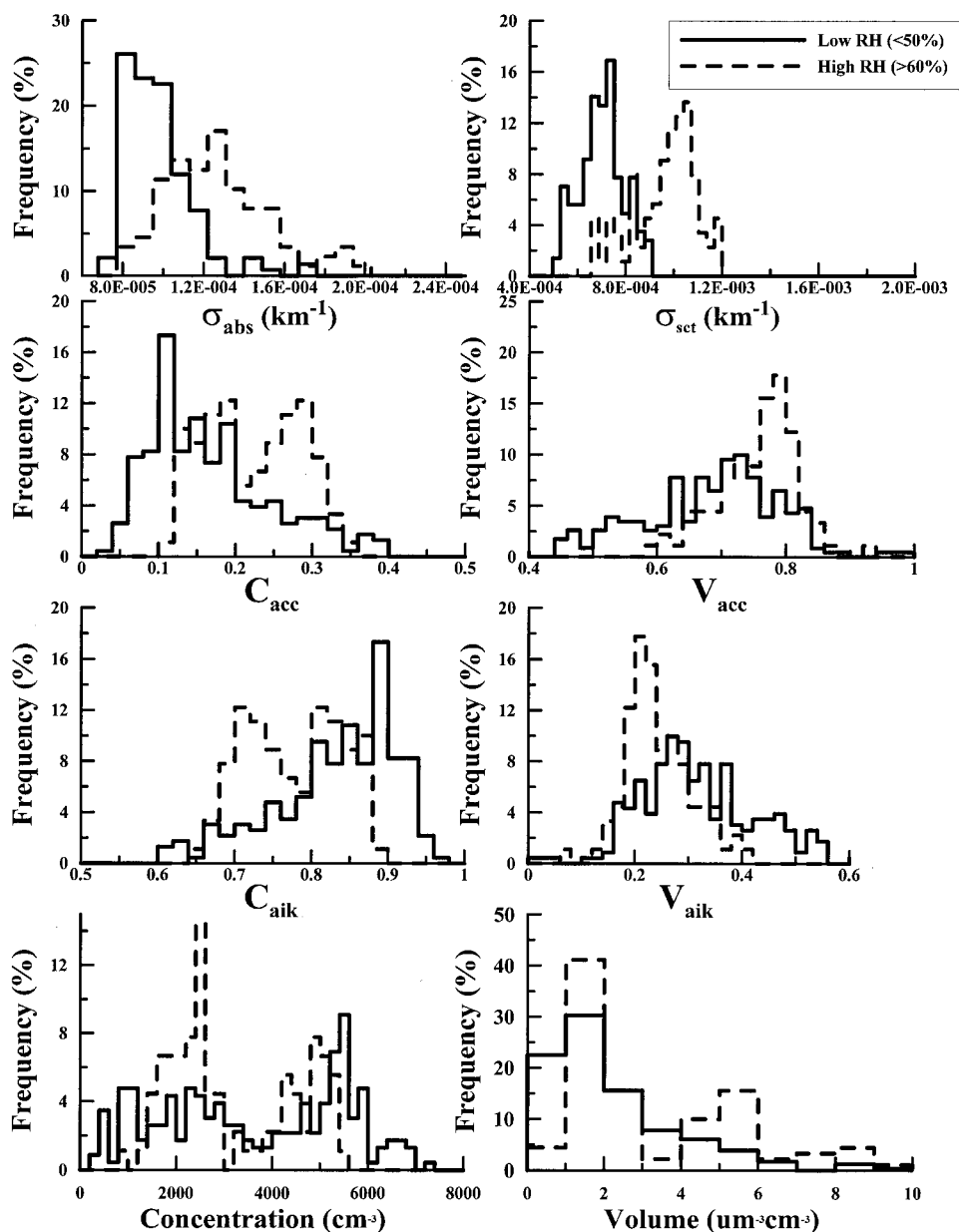
Figure 8. Frequency distributions of the physical and optical properties of the aerosols for the cases of low (<50%, solid curves) and high (>60%, dashed curves) relative humidity are shown.

4. Discussion

The observations highlight a number of important features in the aerosol properties that are related to processes that produce these particles and affect their evolution. The stratification by Aitken and accumulation mode fractions highlights shifts in aerosol sizes within each day and during the total research period. An increase in C_{Aik} and V_{Aik} can be caused by new particle formation, evaporation of accumulation mode particles, or changing air mass, i.e., arrival of air whose aerosols are less aged. A decrease in C_{Aik} and V_{Aik} with a resulting increase in C_{acc} and V_{acc} is a result of growing Aitken mode particles or a change in air mass where the particles have had longer to age. In the morning, before the arrival of city air at the research site, CO is low, but aerosol concentrations and light-scattering coefficients are moderately high. The aerosol

measurements from November 15 and 16 show that CO, the best tracer for city air, decreases at night to low levels, but the particle concentration remains near 2000 cm^{-3} with an associated scattering coefficient also quite high at 7×10^{-4} m^{-1}. The high nighttime aerosol concentration and downslope winds suggest that particles are being transported from aloft. The high O_3 values at nighttime are a result of this transport process, as was shown by *Raga et al.* [1999a].

CO and aerosols, particularly elemental and organic carbon particles, are produced by combustion, i.e., car and truck traffic and many types of industrial processes. There is never a lull in the vehicular traffic in Mexico City, but it peaks during morning and evening rush hours. The positive correlation between CO and the absorption and scattering coefficients measured at the research site, and the increase in C_{Aik} with the morning
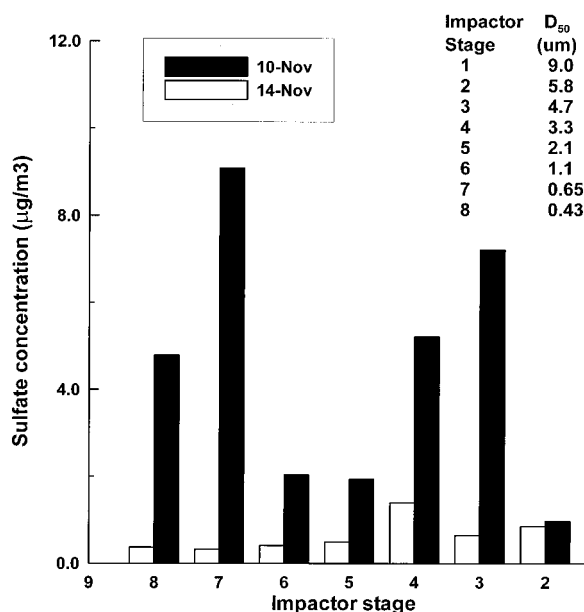
Figure 9. Sulfate mass concentrations as a function of impactor stage of the Andersen impactor are presented here for a day with high RH (solid bars, November 10) and one with low RH (open bars, November 14). The cut sizes listed are nominal on the basis of manufacturer specifications.

arrival of city air, indicates that a large fraction of the measured particles are from primary emissions. The chemical analysis shows that OC and EC constitute approximately 40% of the mass in particles less than a micrometer in diameter. The O_3 increase that follows the initial peak in CO occurs as the
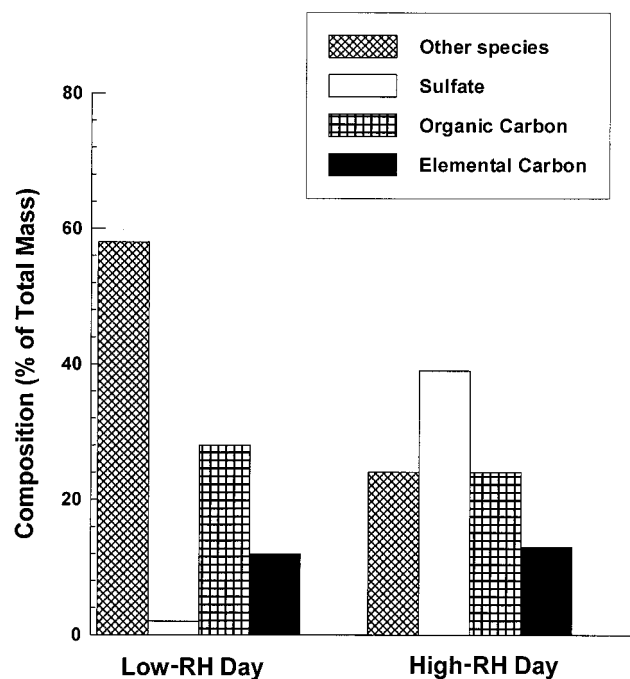

Figure 10. The low- and high-RH days had similar fractions of total carbon, in both organic and elemental form. The amount of sulfate on the high-RH day is significantly larger than that on the low-RH day.

mixed layer develops past the research site and brings more aged aerosols. This is seen as an increase in C_{acc} and V_{acc} when O_3 increases.

The maximum particle concentrations were lower than expected for an urban environment; however, it is likely that mixing and dilution greatly reduce the initial aerosol population emitted in the city. This type of reduction has been seen by others, e.g., *Väkevä et al.* [1999], who showed that particle concentrations are reduced by as much as a factor of 5 between the street level and a building top 25 m above. *Harrison et al.* [1999] found that aerosol concentrations next to a busy highway were on the order of 80,000 cm^{-3}, but downwind by only 350 m they had been reduced to less than 10,000 cm^{-3}. They concluded that the decrease was attributable primarily to mixing and dilution.

The effect of humidity on aerosol properties is seen as an increase in the amount of sulfate on the particles and an associated increase in the fraction of concentration and mass in accumulation mode particles. Sulfur dioxide is highly soluble in water, so that hydrated aerosols provide a very efficient mechanism by which SO_2 is converted to sulfate on these particles [*Seinfeld and Pandis*, 1998]. Various organic compounds found in the urban environment are also soluble in water, so that condensation of these compounds likely proceeds faster on hydrated particles than on dry aerosols. The general effect is that the initial Aitken mode particles grow into the accumulation size range more rapidly under high-humidity conditions than when RH is low. This is reflected in the increased light scattering, since the scattering coefficient is more sensitive to changes in volume than to variations in number concentration.

5. Summary and Conclusions

Measurements of the chemical, physical, and optical properties of aerosols during a pilot project in Mexico City have provided a wealth of information about the properties of particles in this very large urban area. The chemical analysis of these aerosols provides direct evidence that soot, organic compounds, and sulfate dominate their composition, but water vapor and cloud droplets act to control the relative fractions of sulfate that make up their composition. The physical and optical properties are likewise altered by the relative abundance of water in both the gas and liquid phases and must be taken into account when assessing the subsequent impact of these aerosols on the environment. Changes in the partitioning of particle sizes between the Aitken and accumulation modes are correlated with CO and ozone, linking the evolution of aerosols with primary emissions and condensational growth. Further studies are needed, however, to better understand the physical mechanisms by which Aitken mode particles evolve into larger sizes.

The presence at nighttime of large ozone and aerosol concentrations at the elevated research site is important. Although these concentrations could be natural background levels in this region, they might also indicate a source of pollutants that result from recirculation in the city basin that will further impact pollution levels in the region.

The results of this study are applicable to large urban areas since Mexico City is similar to many of the other "megacities" of the world; however, more extensive studies are needed to better understand the mechanisms of aerosol formation and growth before steps can be taken to reduce the levels of aerosols in these cities.

References

Aldape, F., J. Flores, and R. V. Diaz, Seasonal study of the composition of atmospheric aerosols in Mexico City, *Int. J. PIXIE*, *1*, 355–371, 1991a.

Aldape, F., J. Flores, and R. V. Diaz, Two year study of elemental composition of atmospheric aerosols in Mexico City, *Int. J. PIXIE*, *1*, 373–388, 1991b.

Bond, T. C., T. L. Anderson, and D. Cambell, Calibration and intercomparison of filter-based measurements of visible light absorption by aerosols, *Aerosol Sci. Technol.*, *30*, 582–600, 1999.

Cahill, T. A., R. Morales, and J. Miranda, Comparative aerosol studies of Pacific rim cities: Santiago, Chili (1987); Mexico City, Mexico (1987–1990); and Los Angeles, USA (1973 and 1987), *Atmos. Environ.*, *5*, 747–749, 1996.

Dickerson, R., S. Kondragunta, G. Stenchikov, K. Civerolo, B. Doddridge, and B. Holben, The impact of aerosols on solar UV radiation and photochemical smog, *Science*, *278*, 827–830, 1997.

Dockery, D. W., J. Schwarz, and J. D. Spengler, Air pollution and daily mortality; associations with particulates and acid aerosols, *Environ. Res.*, *59*, 362–373, 1992.

Dockery, D., W. C. A. Pope, X. Xu, J. D. Spengler, J. H. Ware, M. E. Fay, B. G. Ferris Jr., and F. E. Speizer, An association between air pollution and mortality in six U.S. cities, *N. Engl. J. Med.*, *329*, 1753–1759, 1993.

Edgerton, S. J., et al., Particle air pollution in Mexico City: A collaborative research project, *J. Air Waste Manage. Assoc.*, *49*, 1221–1229, 1999.

Fuller, K. A., W. C. Malm, and S. M. Kreidenweis, Effects of mixing on extinction by carbonaceous particles, *J. Geophys. Res.*, *104*, 15,941–15,954, 1999.

Goldberg, E. D., *Black Carbon in the Environment*, John Wiley, New York, 1985.

Harrison, R. M., J. Ping Shi, and M. R. Jones, Continuous measurements of aerosol physical properties in the urban atmosphere, *Atmos. Environ.*, *33*, 1037–1047, 1999.

International Agency for Research on Cancer (IARC), *Diesel and Gasoline Engine Exhausts and Some Nitroarenes*, IARC Mongr. Eval. Carcinog. Risk Chem. Hum., *46*, 1989.

Knox, J. B., View from the center: Supercities conference, *Atmos. Environ.*, *30*, 675–677, 1996.

Mage, D., G. Ozolins, P. Peterson, A. Webster, R. Orthofer, V. Vandeweerd, and M. Gwynne, Urban air pollution in megacities of the world, *Atmos. Environ.*, *30*, 681–686, 1996.

Miranda, J., J. R. Morales, T. A. Cahill, F. Aldape, and J. Flores, A study of elemental contents in atmospheric aerosols in Mexico City, *Atmosfera*, *5*, 95–108, 1992.

Novakov, T., Microchemical characterization of aerosols, in *Nature, Aim and Methods of Microchemistry: Proceedings of the 8th International Symposium*, organized by the Austrian Society for Microchemistry and Analytical Chemistry Graz, August 25–30, 1980, edited by H. Malissa, M. Grasserbauer, and R. Belcher, pp. 141–165, Springer-Verlag, New York, 1981.

Pitts, J. N., Jr., Formation and fate of gaseous and particulate mutagens and carcinogens in real and simulated atmospheres, *Environ. Health Perspect.*, *47*, 115–140, 1983.

Raga, G. B., and A. C. Raga, On the formation of an elevated ozone peak in Mexico City, *Atmos. Environ.*, *34*, 4097–4102, 2000.

Raga, G. B., D. Baumgardner, G. Kok, and I. Rosas, Some aspects of boundary layer evolution in Mexico City, *Atmos. Environ.*, *33*, 5013–5021, 1999a.

Raga, G. B., G. Kok, D. Baumgardner, I. Rosas, and A. Báez, Evidence for volcanic influence on Mexico City particulates, *Geophys. Res. Lett.*, *26*, 1149–1152, 1999b.

Schuetzle, D., Sampling of vehicle emissions for chemical analysis and biological testing, *Environ. Health Perspect.*, *47*, 65–80, 1983.

Seila, G. E., W. A. Lonneman, M. E. Ruiz, and J. Tejeda, VOCs in Mexico City ambient air, paper presented at International Symposium on Measurement of Toxic and Related Air Pollutants, Air and Waste Manage. Assoc., Durham, N. C., 1993.

Seinfeld, J. H., and S. N. Pandis, *Atmospheric Chemistry and Physics*, 1326 pp., John Wiley, New York, 1998.

Väkevä, M., K. Hämeri, M. Kulmala, R. Lahdes, J. Ruuskanen, and T. Laitinen, Street level rooftop concentrations of submicron aerosol particles and gaseous pollutants in an urban street canyon, *Atmos. Environ.*, *33*, 1385–1397, 1999.

World Health Organization, United Nations Environment Programme, (WHO UNEP), *Urban Air Pollution in Megacities of the World*, Blackwell, Malden, Mass., 1992.

———
A. Báez, D. Baumgardner, G. B. Raga, and I. Rosas, Centro de Ciencias de la Atmósfera, Universidad Nacional Autónoma de Mexico, Circuito Exterior, Ciudad Universitaria, 04510 Mexico City, DF, Mexico. (darrel@servidor.unam.mx; raga@servidor.unam.mx)

G. Kok, National Center for Atmospheric Research, Box 3000, Boulder, CO 80307. (kok@ucar.edu)

T. Novakov, Atmospheric Aerosol Research, Lawrence Berkeley National Laboratory, University of California, Berkeley, 1 Cyclotron Road, Building 73, Berkeley, CA 94720. (tnovakov@lbl.gov)

J. Ogren, NOAA/CMDL, 325 Broadway, R/E/CG1, Boulder, CO 80303-3328. (jogren@cmdl.noaa.gov)